Progress In Electromagnetics Research, PIER 38, 125–146, 2002

MAGNETIC POTENTIAL GREEN'S DYADICS OF MULTILAYERED WAVEGUIDE FOR SPATIAL POWER COMBINING APPLICATIONS

M. V. Lukic and A. B. Yakovlev

Department of Electrical Engineering
The University of Mississippi
University, MS 38677-1848, USA

Abstract—Integral equation formulation and magnetic potential Green's dyadics for multilayered rectangular waveguide are presented for modeling interacting printed antenna arrays used in waveguide-based spatial power combiners. Dyadic Green's functions are obtained as a partial eigenfunction expansion in the form of a double series over the complete system of eigenfunctions of transverse Laplacian operator. In this expansion, one-dimensional characteristic Green's functions along a multilayered waveguide are derived in closed form as the solution of a Sturm-Liouville boundary value problem with appropriate boundary and continuity conditions. A method introduced here is based on the transmission matrix approach, wherein the amplitude coefficients of forward and backward traveling waves in the scattered Green's function in different dielectric layers are obtained as a product of transmission matrices of corresponding layers. Convergence of Green's function components in the source region is illustrated for a specific example of a two-layered, terminated rectangular waveguide.

1. INTRODUCTION

Dyadic Green's functions (DGFs) play a significant role in integral equation methods used in the analysis of various electromagnetic wave propagation and scattering problems [1, 2]. In the past few decades, considerable amount of research has been devoted to the development of DGFs of rectangular waveguides and cavities [1–14]. They are traditionally constructed in the form of a double series expansion using the Hansen vector wave functions [1–10]. Thus, electric and magnetic DGFs for an infinite and semi-infinite rectangular waveguide and rectangular cavity were obtained in [1–3]. In [4], several different but equivalent representations of DGFs for a rectangular cavity were obtained, and the mathematical relations between the DGF of the vector (magnetic) potential type and that of the electric type were shown in detail. A hybrid ray-mode representation of the Green's function in an overmoded rectangular cavity was developed in [5], using the finite Poisson's summation formula. DGFs for a rectangular waveguide with an E-plane dielectric slab were derived in [6] based the Ohm-Rayleigh method. In [7], rectangular waveguide Green's function involving full-wave discrete complex images was proposed for the analysis of waveguide discontinuity problems. A rigorous Green's function analysis of rectangular microstrip patch antennas enclosed in a rectangular cavity was developed in [8]. A rapid calculation scheme based on the Ewald's sum technique was proposed in [9] for the potential Green's functions of the rectangular waveguide. An image-spectral approach was used in [10] to derive the computationally efficient expressions of the DGFs for rectangular enclosures.

There has also been work on DGFs for a multilayered rectangular waveguide [11, 12]. In [11], the electric DGF for a rectangular waveguide filled with longitudinally multilayered isotropic dielectric was obtained using the method of mode expansion and scattering superposition. Electric and magnetic Green's functions for a semi-infinite rectangular waveguide filled with arbitrary multilayered media were presented in [12], where analytical expressions of the scattering DGF coefficients were obtained in terms of transmission matrices using the principle of scattering superposition.

An alternative method of developing Green's dyadics for rectangular waveguides and cavities utilizes a partial eigenfunction expansion

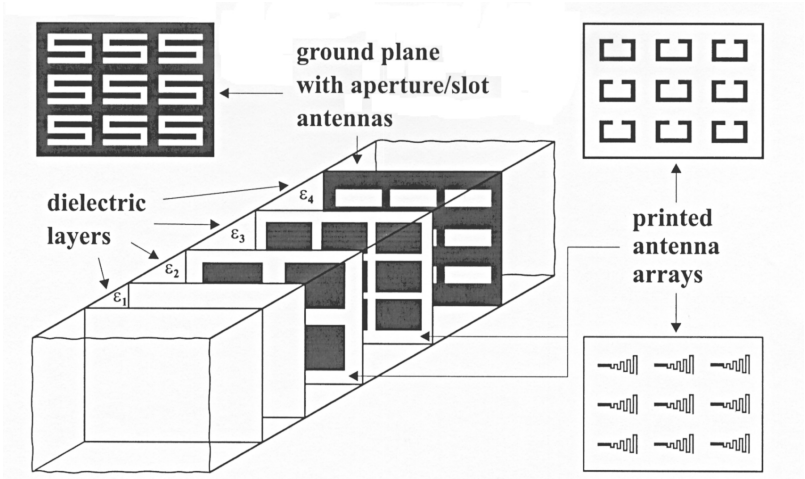

Figure 1. Multilayered waveguide transition containing interacting printed antenna arrays.

as a double series expansion over the complete system of eigenfunctions of the transverse Laplacian operator [13,14]. The unknown coefficients in this expansion represent one-dimensional characteristic Green's functions along the waveguide. The properties of completeness and orthogonality of eigenfunctions in the waveguide cross-section allow for reduction of the three-dimensional problem to a one-dimensional Sturm-Liouville boundary value problem for the unknown characteristic Green's functions. In [14], electric DGFs for a semi-infinite partially filled rectangular waveguide are obtained for the full-wave analysis of a waveguide-based aperture-coupled patch amplifier array. The derived characteristic Green's functions provide a physical insight into resonance and surface wave effects occurring in overmoded layered waveguide transitions.

The work presented here was motivated by the necessity to develop a modeling environment for waveguide-based spatial power combiners, wherein arbitrarily shaped printed antenna arrays are placed at dielectric interfaces of an oversized multilayered rectangular waveguide (Fig. 1). Narrowband resonant rectangular slot antennas used in earlier designs [15, 16] are replaced by meander-slot antennas and their modifications [17, 18], in order to increase the frequency bandwidth and efficiency of the system.

The paper is organized as follows. An integral equation formulation is given in Section 2, where a coupled set of integral equations is obtained for the induced electric and magnetic surface current

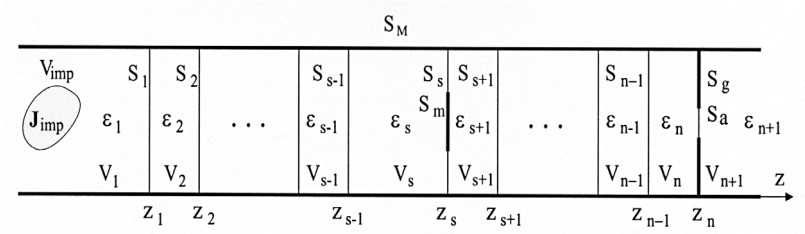

Figure 2. A multilayered waveguide-based transition module.

densities. In this paper we primarily concentrate on the development of magnetic potential DGFs for a multilayered rectangular waveguide with an arbitrarily oriented point source. Thus, in Section 3 a detailed analysis of DGFs is presented, which is based on the partial eigenfunction expansion of Green's function components in conjunction with a proposed transmission matrix approach. In this method, one-dimensional characteristic Green's functions along a multilayered waveguide are obtained in closed form as a product of transmission matrices of corresponding layers. Numerical results for convergence of Green's function components are given in Section 4 for a specific example of a two-layered, terminated rectangular waveguide.

2. INTEGRAL EQUATION FORMULATION

Consider a waveguide-based transition module with n dielectric layers shown in Fig. 2. This is a generalized case of the module investigated in [15, 16]. An arbitrarily-shaped metallization S_m (electric layer) and apertures S_a (magnetic layer) in a ground plane are placed at the interfaces of adjacent dielectric layers at $z = z_s$ and $z = z_n$, respectively. The incident electric and magnetic fields in the region V_1 are generated by an impressed electric current source $\mathbf{J}_{imp}$ ($\nabla \times \mathbf{J}_{imp}$ for the magnetic field). The scattered electric and magnetic fields in regions V_i (for $i = 1, 2, ..., n$) are generated by the electric current induced on the metallization S_m and by the magnetic current induced on the surface of slot apertures S_a. The electric and magnetic fields in the region V_{n+1} are due to magnetic currents only, but the continuity of tangential components of the magnetic field across the surface S_a provides the interaction of all regions and necessitates the formulation of the problem in terms of coupled electric- and magnetic-field integral equations.

A coupled set of integral equations is obtained by enforcing a boundary condition for the tangential components of the electric field

on the conducting surface S_m at $z = z_s$,

$$\widehat{z} \times \left(\mathbf{E}_s^{(inc)} (\mathbf{r}) + \mathbf{E}_s^{(scat)} (\mathbf{r}) \right) = 0 \tag{1}$$

and a continuity condition for the tangential components of the magnetic field on the surface of the slot apertures S_a at $z = z_n$,

$$\widehat{z} \times \left(\mathbf{H}_n^{(inc)} (\mathbf{r}) + \mathbf{H}_n^{(scat)} (\mathbf{r}) \right) = \widehat{z} \times \mathbf{H}_{n+1}^{(scat)} (\mathbf{r}) . \tag{2}$$

The integral form of the boundary condition (1) is obtained by combining the vector-wave equation formulation for the electric field and the corresponding formulation for the electric DGF. The integral-equation formulation of the second vector-dyadic Greens theorem [2] with appropriate boundary and continuity conditions results in

$$\begin{aligned} -j\omega\mu_0 \widehat{z} \times \int_{V_{imp}} \mathbf{J}_{imp} (\mathbf{r}') \cdot \underline{\mathbf{G}}_{e1}^{(1s)} (\mathbf{r}', \mathbf{r}) \, dV' \\ = j\omega\mu_0 \widehat{z} \times \int_{S_m} \mathbf{J} (\mathbf{r}') \cdot \underline{\mathbf{G}}_{e1}^{(ss)} (\mathbf{r}', \mathbf{r}) \, dS' \\ - \widehat{z} \times \int_{S_a} \mathbf{M} (\mathbf{r}') \cdot [\nabla' \times \underline{\mathbf{G}}_{e1}^{(ns)} (\mathbf{r}', \mathbf{r})] dS'. \end{aligned} \tag{3}$$

Here, the integral on the left-hand side of (3) is the incident electric field due to an impressed electric current $\mathbf{J}_{imp} (\mathbf{r}')$ and the integrals on the right-hand side are the scattered electric fields due to induced electric $\mathbf{J} (\mathbf{r}')$ and magnetic $\mathbf{M} (\mathbf{r}')$ currents.

The continuity condition for tangential components of the magnetic field (2) is obtained in integral form using a similar procedure as that described above for the electric-field vector resulting in the magnetic-field integral equation for the unknown currents $\mathbf{J} (\mathbf{r}')$ and $\mathbf{M} (\mathbf{r}')$,

$$\begin{aligned} \frac{\varepsilon_n}{\varepsilon_1} \widehat{z} \times \int_{V_{imp}} \left[\nabla' \times \mathbf{J}_{imp} (\mathbf{r}') \right] \cdot \underline{\mathbf{G}}_{e2}^{(1n)} (\mathbf{r}', \mathbf{r}) \, dV' \\ = -\frac{\varepsilon_n}{\varepsilon_s} \widehat{z} \times \int_{S_m} \mathbf{J} (\mathbf{r}') \cdot [\nabla' \times \underline{\mathbf{G}}_{e2}^{(sn)} (\mathbf{r}', \mathbf{r})] dS' \\ - j\omega\varepsilon_0 \widehat{z} \times \int_{S_a} \mathbf{M} (\mathbf{r}') \cdot \left[\varepsilon_n \underline{\mathbf{G}}_{e2}^{(nn)} (\mathbf{r}', \mathbf{r}) + \varepsilon_{n+1} \underline{\mathbf{G}}_{e2}^{(n+1)} (\mathbf{r}', \mathbf{r}) \right] dS' \end{aligned} \tag{4}$$

where $\underline{\mathbf{G}}_{e2}^{(n+1)} (\mathbf{r}, \mathbf{r}')$ is the electric dyadic Green's function of the second kind for a semi-infinite rectangular waveguide filled with dielectric

with permittivity ε_{n+1} and terminated by a ground plane at $z = z_n$ (obtained similar to that presented in [14]). The electric DGFs $\underline{\mathbf{G}}_{e1}^{(is)}$ and $\underline{\mathbf{G}}_{e2}^{(in)}$ (for $i = 1, ..., s, ..., n$), serving as kernels of the integral equations (3) and (4), are obtained from the magnetic potential Green's dyadics $\underline{\mathbf{G}}_{A1}^{(is)}$ and $\underline{\mathbf{G}}_{A2}^{(in)}$ as follows [19],

$$\underline{\mathbf{G}}_{er}^{(il)}\left(\mathbf{r}, \mathbf{r}'\right) = \left(\underline{\mathbf{I}} + \frac{1}{k_i^2}\nabla\nabla\right) \cdot \underline{\mathbf{G}}_{Ar}^{(il)}\left(\mathbf{r}, \mathbf{r}'\right) \tag{5}$$

where $l = s, n$ corresponds to $r = 1, 2$, respectively. Magnetic potential Green's dyadics $\underline{\mathbf{G}}_{A1}^{(is)}\left(\mathbf{r}, \mathbf{r}'\right)$ used in the electric-field integral equation formulation (3) will be obtained in the section to follow, and the formulation for $\underline{\mathbf{G}}_{A2}^{(in)}\left(\mathbf{r}, \mathbf{r}'\right)$ used in the magnetic-field integral equation (4) is given in Appendix A.

3. MAGNETIC POTENTIAL GREEN'S DYADICS FOR A SEMI-INFINITE MULTILAYERED RECTANGULAR WAVEGUIDE

In this section we present a method of deriving the magnetic potential DGF $\underline{\mathbf{G}}_{A1}^{(is)}\left(\mathbf{r}, \mathbf{r}'\right)$ for a semi-infinite multilayered rectangular waveguide used in the electric-field integral equation formulation. The Green's function components are obtained as a partial eigenfunction expansion with a complete basis of eigenfunctions in the waveguide cross-section. Based on the properties of completeness and orthogonality of eigenfunctions a three-dimensional Green's function problem is reduced to a one-dimensional Sturm-Liouville boundary value problem for characteristic Green's functions in the waveguiding direction. Characteristic Green's functions are represented as a superposition of primary and scattered parts subject to appropriate boundary and continuity conditions. In this formulation, scattered parts are obtained in terms of traveling waves (forward and backward) with amplitude coefficients expressed as a product of transmission matrices associated with a multilayered waveguide.

The magnetic potential DGF for a semi-infinite multilayered rectangular waveguide with a point source arbitrarily positioned in region V_s (Fig. 3) satisfies the following dyadic differential equations in regions of dielectric layers V_i, $(i = 1, 2, ..., n)$,

$$\nabla^2 \underline{\mathbf{G}}_{A1}^{(is)}\left(\mathbf{r}, \mathbf{r}'\right) + k_i^2 \underline{\mathbf{G}}_{A1}^{(is)}\left(\mathbf{r}, \mathbf{r}'\right) = -\delta_{is}\underline{\mathbf{I}}\delta\left(\mathbf{r} - \mathbf{r}'\right), \quad \mathbf{r} \in V_i,\ \mathbf{r}' \in V_s \tag{6}$$

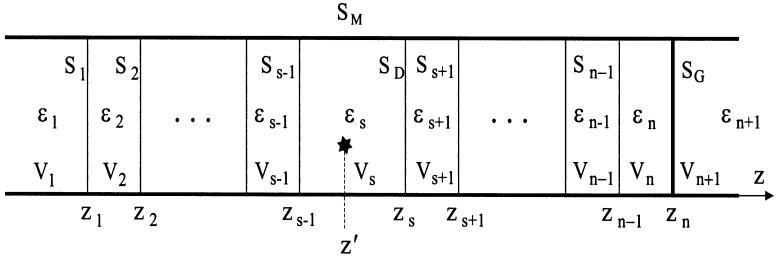

Figure 3. Multilayered semi-infinite waveguide with an arbitrarily oriented point source located in the region V_s.

subject to boundary conditions of the first kind on the waveguide surface S_M and surface of the ground plane $S_G = S_g \cup S_a$,

$$\begin{aligned} \hat{n} \times \underline{\mathbf{G}}_{A1}^{(is)}(\mathbf{r}, \mathbf{r}') &= 0, \quad \mathbf{r} \in S_M \cup S_G \\ \nabla \cdot \underline{\mathbf{G}}_{A1}^{(is)}(\mathbf{r}, \mathbf{r}') &= 0, \quad \mathbf{r} \in S_M \cup S_G \end{aligned} \tag{7}$$

and mixed continuity conditions of the third kind across the dielectric interfaces S_q (for $q = 1, 2, ..., n-1$),

$$\begin{aligned} \hat{z} \times \underline{\mathbf{G}}_{A1}^{(qs)}(\mathbf{r}, \mathbf{r}') &= \hat{z} \times \underline{\mathbf{G}}_{A1}^{(q+1s)}(\mathbf{r}, \mathbf{r}'), & \mathbf{r} \in S_q \\ \hat{z} \cdot \underline{\mathbf{G}}_{A1}^{(qs)}(\mathbf{r}, \mathbf{r}') &= \hat{z} \cdot \underline{\mathbf{G}}_{A1}^{(q+1s)}(\mathbf{r}, \mathbf{r}'), & \mathbf{r} \in S_q \\ \hat{z} \times \nabla \times \underline{\mathbf{G}}_{A1}^{(qs)}(\mathbf{r}, \mathbf{r}') &= \hat{z} \times \nabla \times \underline{\mathbf{G}}_{A1}^{(q+1s)}(\mathbf{r}, \mathbf{r}'), & \mathbf{r} \in S_q \\ \frac{1}{\varepsilon_q} \nabla \cdot \underline{\mathbf{G}}_{A1}^{(qs)}(\mathbf{r}, \mathbf{r}') &= \frac{1}{\varepsilon_{q+1}} \nabla \cdot \underline{\mathbf{G}}_{A1}^{(q+1s)}(\mathbf{r}, \mathbf{r}'), & \mathbf{r} \in S_q. \end{aligned} \tag{8}$$

The solution of the boundary value problem (6)–(8) yields nine components of the magnetic Green's dyadics expressed as a partial eigenfunction expansion,

$$G_{\alpha\beta,A1}^{(is)}(x, y, z, x', y', z') = \sum_{m=0}^{\infty} \sum_{n=0}^{\infty} \phi_{mn}^{\alpha}(x, y) \, \phi_{mn}^{\beta}(x', y') \, f_{mn,\alpha\beta}^{(is)}(z, z'), \tag{9}$$

for $\alpha, \beta = x, y, z$, where $\phi_{mn}^{\alpha}(x, y)$ form a complete basis of orthonormal eigenfunctions of the transverse Laplacian operator in the

waveguide cross-section ($a \times b$),

$$\begin{aligned}
\phi^{x}_{mn}(x,y) &= \sqrt{\frac{\varepsilon_{0m}\varepsilon_{0n}}{ab}}\cos(k_x x)\sin(k_y y),\\
\phi^{y}_{mn}(x,y) &= \sqrt{\frac{\varepsilon_{0m}\varepsilon_{0n}}{ab}}\sin(k_x x)\cos(k_y y), \qquad (10)\\
\phi^{z}_{mn}(x,y) &= \sqrt{\frac{\varepsilon_{0m}\varepsilon_{0n}}{ab}}\sin(k_x x)\sin(k_y y),
\end{aligned}$$

with k_x and k_y being the transverse eigenvalues such that $k_x = \frac{m\pi}{a}$, $k_y = \frac{n\pi}{b}$. Here, a and b are the waveguide dimensions in the x- and y-direction, respectively, and $f^{(is)}_{mn,\alpha\beta}(z,z')$ are the one-dimensional characteristic Green's functions in the waveguiding direction. In (10), ε_{0m} and ε_{0n} are the Neumann indexes, such that $\varepsilon_{00} = 1$ and $\varepsilon_{0m} = 2$ when $m \neq 0$.

The use of the eigenfunction expansion (9) reduces the three-dimensional boundary value problem (6)–(8) to a one-dimensional Sturm-Liouville boundary value problem for the characteristic Green's functions,

$$\frac{\partial^2}{\partial z^2} f^{(is)}_{mn,\alpha\beta}(z,z') - \gamma_i^2 f^{(is)}_{mn,\alpha\beta}(z,z') = -\delta_{is}\delta_{\alpha\beta}\delta(z-z'), \quad z_{i-1} < z < z_i, \qquad (11)$$

$$f^{(ns)}_{mn,x\beta}(z_n,z') = f^{(ns)}_{mn,y\beta}(z_n,z') = \frac{\partial}{\partial z} f^{(ns)}_{mn,z\beta}(z_n,z') = 0, \qquad (12)$$

$$\begin{aligned}
f^{(qs)}_{mn,\alpha\beta}(z_q,z') &= f^{(q+1s)}_{mn,\alpha\beta}(z_q,z'),\\
\frac{\partial}{\partial z} f^{(qs)}_{mn,x\beta}(z_q,z') &= \frac{\partial}{\partial z} f^{(q+1s)}_{mn,x\beta}(z_q,z'), \qquad (13)\\
\frac{\partial}{\partial z} f^{(qs)}_{mn,y\beta}(z_q,z') &= \frac{\partial}{\partial z} f^{(q+1s)}_{mn,y\beta}(z_q,z'),
\end{aligned}$$

$$\frac{1}{\varepsilon_q}\left[-k_x f^{(qs)}_{mn,x\beta}(z_q,z') - k_y f^{(qs)}_{mn,y\beta}(z_q,z') + \frac{\partial}{\partial z} f^{(qs)}_{mn,z\beta}(z_q,z')\right] = \frac{1}{\varepsilon_{q+1}}\left[-k_x f^{(q+1s)}_{mn,x\beta}(z_q,z') - k_y f^{(q+1s)}_{mn,y\beta}(z_q,z') + \frac{\partial}{\partial z} f^{(q+1s)}_{mn,z\beta}(z_q,z')\right],$$

where $i = 1, 2, ..., n$, $q = 1, 2, ..., n-1$, and γ_i is the propagation constant of propagating and evanescent waveguide modes in regions V_i,

$$\gamma_i = \begin{cases} j\sqrt{k_i^2 - k_x^2 - k_y^2}, & k_i^2 > k_x^2 + k_y^2 \\ \sqrt{k_x^2 + k_y^2 - k_i^2}, & k_i^2 < k_x^2 + k_y^2 \end{cases}.$$

The solution of the system of differential equations (11) is obtained as a superposition of the primary and scattered parts,

$$\begin{aligned} & f_{mn,\alpha\beta}^{(is)}\left(z, z'\right) \\ & = \delta_{is}\delta_{\alpha\beta}\frac{e^{-\gamma_s|z-z'|}}{2\gamma_s} + (1-\delta_{i1})\, A_{\alpha\beta}^{(is)} e^{-\gamma_i(z-z_{i-1})} + B_{\alpha\beta}^{(is)} e^{\gamma_i(z-z_i)} \end{aligned} \quad (14)$$

where the first term (primary part) is the one-dimensional Green's function of an infinite waveguide and two other terms (scattered part) represent forward and backward traveling waves in waveguide regions V_i. The unknown coefficients $A_{\alpha\beta}^{(is)}$ and $B_{\alpha\beta}^{(is)}$ will be determined in closed form subject to boundary and continuity conditions (12) and (13).

The use of the representation (14) and continuity conditions (13) gives $f_{mn,xy}^{(is)}(z, z') = f_{mn,xz}^{(is)}(z, z') = f_{mn,yx}^{(is)}(z, z') = f_{mn,yz}^{(is)}(z, z') = 0$. Therefore, only five out of nine magnetic DGFs components are non-zero:

$$\underline{\mathbf{G}}_{A1}^{(is)} = \begin{bmatrix} G_{xx,A1}^{(is)} & 0 & 0 \\ 0 & G_{yy,A1}^{(is)} & 0 \\ G_{zx,A1}^{(is)} & G_{zy,A1}^{(is)} & G_{zz,A1}^{(is)} \end{bmatrix}.$$

The solution for characteristic Green's functions $f_{mn,xx}^{(is)}(z, z')$ and $f_{mn,zx}^{(is)}(z, z')$ will be given first, followed by the solution for the function $f_{mn,zz}^{(is)}(z, z')$. For the sake of brevity, the solution for functions $f_{mn,yy}^{(is)}(z, z')$ and $f_{mn,zy}^{(is)}(z, z')$ is excluded. It can be obtained using a similar procedure to that for functions $f_{mn,xx}^{(is)}(z, z')$ and $f_{mn,zx}^{(is)}(z, z')$ by interchanging x and y variables.

By the representation (14), functions $f_{mn,xx}^{(is)}(z, z')$ and $f_{mn,zx}^{(is)}(z, z')$ are expressed in terms of coefficients $\left[\begin{smallmatrix} A_{xx}^{(is)} & B_{xx}^{(is)} \end{smallmatrix}\right]$ and $\left[\begin{smallmatrix} A_{zx}^{(is)} & B_{zx}^{(is)} \end{smallmatrix}\right]$, respectively. We now introduce vectors of unknown coefficients $\mathbf{C}_x^{(is)} =$

$\left[\, A_{xx}^{(is)}\ B_{xx}^{(is)}\ A_{zx}^{(is)}\ B_{zx}^{(is)} \,\right]^T$, $i = 1, 2, ..., n$, where T denotes transpose operation. Note that $A_{xx}^{(1s)} = A_{zx}^{(1s)} = 0$, such that $\mathbf{C}_x^{(1s)} = \left[\, 0\ B_{xx}^{(1s)}\ 0\ B_{zx}^{(1s)} \,\right]^T$. This results in $4n-2$ unknown coefficients A and B introduced in the characteristic functions $f_{mn,xx}^{(is)}(z, z')$ and $f_{mn,zx}^{(is)}(z, z')$. Each of the continuity conditions (13), for $q = 1, 2, ..., n-1$, provides four equations for these coefficients, and the boundary condition (12) provides two additional equations. Instead of solving the system of $4n-2$ equations for $4n-2$ unknown coefficients by brute force, we propose a method of reducing this system to a system of only four equations for the four key unknown coefficients, $B_{xx}^{(1s)}$, $B_{zx}^{(1s)}$, $A_{xx}^{(ns)}$and $A_{zx}^{(ns)}$, and expressing all other coefficients in terms of these four. It is convenient to group these four key coefficients into vectors $\mathbf{B}_x^{(1s)} = \left[\, B_{xx}^{(1s)}\ B_{zx}^{(1s)} \,\right]^T$ and $\mathbf{A}_x^{(ns)} = \left[\, A_{xx}^{(ns)}\ A_{zx}^{(ns)} \,\right]^T$. Coefficients $\mathbf{C}_x^{(is)}$ will then be expressed in terms of $\mathbf{B}_x^{(1s)}$, for $i = 1, ..., s-1, s$, and in terms of $\mathbf{A}_x^{(ns)}$, for $i = s, s+1, ..., n$. Note that the coefficients $\mathbf{C}_x^{(ss)}$ have two different representations: one in terms of $\mathbf{B}_x^{(1s)}$ and another one in terms of $\mathbf{A}_x^{(ns)}$.

The representation (14) subject to the boundary and continuity conditions (12), (13) results in the expressions for coefficients $\mathbf{C}_x^{(is)}$ in terms of the key coefficients $\mathbf{B}_x^{(1s)}$,

$$\begin{aligned} \mathbf{C}_x^{(1s)} &= \Theta_x^1 \cdot \mathbf{B}_x^{(1s)}, \\ \mathbf{C}_x^{(is)} &= \mathbf{L}_x^i \cdot \mathbf{B}_x^{(1s)} - \frac{\delta_{is}}{2\gamma_s E_s} \left[0 \quad 1 \quad 0 \quad 0\right]^T, \end{aligned} \tag{15}$$

where $E_s = e^{-\gamma_s(z_s - z')}$, and matrices Θ_x^1 and $\mathbf{L}_x^i$ are obtained as

$$\Theta_x^1 = \begin{bmatrix} 0 & 1 & 0 & 0 \\ 0 & 0 & 0 & 1 \end{bmatrix}^T,$$

and $\mathbf{L}_x^i = \Theta_x^{i,i-1} \cdot \Theta_x^{i-1,i-2} \cdots \Theta_x^{2,1} \cdot \Theta_x^1$, with $\Theta_x^{j+1,j}$ being a transmission matrix such that

$$\Theta_x^{j+1,j} = \frac{1}{2T_{j+1}\varepsilon_j\gamma_{j+1}} \begin{bmatrix} T_{j+1}\varepsilon_j\left(\gamma_{j+1}+\gamma_j\right)T_j & T_{j+1}\varepsilon_j\left(\gamma_{j+1}-\gamma_j\right) & 0 & 0 \\ \varepsilon_j\left(\gamma_{j+1}-\gamma_j\right)T_j & \varepsilon_j\left(\gamma_{j+1}+\gamma_j\right) & 0 & 0 \\ T_{j+1}\left(\varepsilon_{j+1}-\varepsilon_j\right)k_x T_j & T_{j+1}\left(\varepsilon_{j+1}-\varepsilon_j\right)k_x & T_{j+1}\left(\varepsilon_j\gamma_{j+1}+\varepsilon_{j+1}\gamma_j\right)T_j & T_{j+1}\left(\varepsilon_j\gamma_{j+1}-\varepsilon_{j+1}\gamma_j\right) \\ -\left(\varepsilon_{j+1}-\varepsilon_j\right)k_x T_j & -\left(\varepsilon_{j+1}-\varepsilon_j\right)k_x & \left(\varepsilon_j\gamma_{j+1}-\varepsilon_{j+1}\gamma_j\right)T_j & \left(\varepsilon_j\gamma_{j+1}+\varepsilon_{j+1}\gamma_j\right) \end{bmatrix},$$

for $j = 1, 2, ..., n-1$, where $T_i = e^{-\gamma_i(z_i - z_{i-1})}$. The above form of the transmission matrix $\Theta_x^{j+1,j}$ is easily obtained by expressing the continuity condition (13) in matrix form at dielectric interface at $z = z_j$, and the matrix Θ_x^1 is obtained using the equation $\mathbf{C}_x^{(1s)} = \left[0 \; B_{xx}^{(1s)} \; 0 \; B_{zx}^{(1s)}\right]^T$.

Similarly, the representation (14) with the boundary and continuity conditions (12), (13) results in the representation of $\mathbf{C}_x^{(is)}$ in terms of the key coefficients $\mathbf{A}_x^{(ns)}$,

$$\begin{aligned} \mathbf{C}_x^{(ns)} &= \Theta_x^n \cdot \mathbf{A}_x^{(ns)}, \\ \mathbf{C}_x^{(is)} &= \mathbf{R}_x^i \cdot \mathbf{A}_x^{(ns)} - \frac{\delta_{is} E_s}{2\gamma_s T_s} \left[1 \quad 0 \quad 0 \quad 0\right]^T, \end{aligned} \tag{16}$$

where matrices Θ_x^n and $\mathbf{R}_x^i$ are obtained in the form

$$\Theta_x^n = \begin{bmatrix} 1 & -T_n & 0 & 0 \\ 0 & 0 & 1 & T_n \end{bmatrix}^T,$$

and $\mathbf{R}_x^i = (\Theta_x^{i+1,i})^{-1} \cdot (\Theta_x^{i+2,i+1})^{-1} \cdots (\Theta_x^{n,n-1})^{-1} \cdot \Theta_x^n$. The above form of the transmission matrix Θ_x^n is easily obtained by expressing the boundary condition (12) in matrix form at the ground plane at $z = z_n$.

Equating the two different expressions for $\mathbf{C}_x^{(ss)}$, (15) and (16), one obtains the following system of equations for the four key unknown coefficients,

$$\begin{bmatrix} R^s_{x[1,1]} & 0 & -L^s_{x[1,1]} & 0 \\ R^s_{x[2,1]} & 0 & -L^s_{x[2,1]} & 0 \\ R^s_{x[3,1]} & R^s_{x[3,2]} & -L^s_{x[3,1]} & -L^s_{x[3,2]} \\ R^s_{x[4,1]} & R^s_{x[4,2]} & -L^s_{x[4,1]} & -L^s_{x[4,2]} \end{bmatrix} \cdot \begin{bmatrix} A_{xx}^{(ns)} \\ A_{zx}^{(ns)} \\ B_{xx}^{(1s)} \\ B_{zx}^{(1s)} \end{bmatrix} = \frac{1}{2\gamma_s} \begin{bmatrix} \frac{E_s}{T_s} \\ -\frac{1}{E_s} \\ 0 \\ 0 \end{bmatrix} \tag{17}$$

where $R^s_{x[i,j]}$ and $L^s_{x[i,j]}$ (for $i = 1, 2, 3, 4$ and $j = 1, 2$) denote elements of matrices $\mathbf{R}_x^s$ and $\mathbf{L}_x^s$, respectively.

Once the system (17) is solved for $\left[A_{xx}^{(ns)} \; A_{zx}^{(ns)} \; B_{xx}^{(1s)} \; B_{zx}^{(1s)}\right]^T$, the remaining coefficients of the representation (14) are obtained from (15) and (16). Note that the presented procedure holds for cavities and infinite waveguides as well as semi-infinite waveguides terminated from either side. Waveguide terminations are accounted for in the procedure by matrices Θ_x^1 and Θ_x^n which are easily obtained for any of the termination cases by using the above approach for the case of a semi-infinite waveguide.

In addition, when the point source is located in the first dielectric layer ($s = 1$), by making use of equations (16) and $A_{xx}^{(11)} = A_{zx}^{(11)} = 0$, one obtains

$$\begin{bmatrix} R_{x[1,1]}^{1} & 0 \\ R_{x[3,1]}^{1} & R_{x[3,2]}^{1} \end{bmatrix} \cdot \begin{bmatrix} A_{xx}^{(n1)} \\ A_{zx}^{(n1)} \end{bmatrix} = \frac{1}{2\gamma_1} \begin{bmatrix} \frac{E_1}{T_1} \\ 0 \end{bmatrix}. \tag{18}$$

Once this system is solved for the vector of key coefficients $\mathbf{A}_x^{(n1)} = \left[A_{xx}^{(n1)} \; A_{zx}^{(n1)} \right]^T$, the remaining coefficients are obtained from equations (16).

When the point source is positioned in the last dielectric layer ($s = n$), using the equations (15) and $f_{mn,xx}^{(ns)}(z_n, z') = \frac{\partial}{\partial z} f_{mn,zx}^{(ns)}(z_n, z') = 0$, we obtain

$$\begin{bmatrix} L_{x[2,1]}^{n} + T_n L_{x[1,1]}^{n} & 0 \\ L_{x[4,1]}^{n} - T_n L_{x[3,1]}^{n} & L_{x[4,2]}^{n} - T_n L_{x[3,2]}^{n} \end{bmatrix} \begin{bmatrix} B_{xx}^{(1n)} \\ B_{zx}^{(1n)} \end{bmatrix} = \frac{1}{2\gamma_n} \begin{bmatrix} \frac{1}{E_n} - E_n \\ 0 \end{bmatrix}. \tag{19}$$

Once the system (19) is solved for the key coefficients $B_{xx}^{(1n)}$ and $B_{zx}^{(1n)}$, the remaining coefficients can be obtained from (15).

In this part of the paper a procedure of deriving a longitudinal component of the characteristic Green's function, $f_{mn,zz}^{(is)}(z, z')$, is described. Corresponding boundary and continuity conditions (12), (13) are obtained as follows,

$$\frac{\partial}{\partial z} f_{mn,zz}^{(ns)}\left(z_n, z'\right) = 0, \tag{20}$$

$$\begin{aligned} f_{mn,zz}^{(qs)}\left(z_q, z'\right) &= f_{mn,zz}^{(q+1s)}\left(z_q, z'\right), \\ \frac{1}{\varepsilon_q} \frac{\partial}{\partial z} f_{mn,zz}^{(qs)}\left(z_q, z'\right) &= \frac{1}{\varepsilon_{q+1}} \frac{\partial}{\partial z} f_{mn,zz}^{(q+1s)}\left(z_q, z'\right), \end{aligned} \tag{21}$$

where $q = 1, 2, ..., n-1$.

By the representation (14), functions $f_{mn,zz}^{(is)}(z, z')$ are expressed in terms of coefficients $A_{zz}^{(is)}$ and $B_{zz}^{(is)}$. We now introduce vectors of unknown coefficients $\mathbf{C}_z^{(is)}$ containing coefficients $A_{zz}^{(is)}$ and $B_{zz}^{(is)}$, as $\mathbf{C}_z^{(is)} = \left[A_{zz}^{(is)} \; B_{zz}^{(is)} \right]^T$. Note that $A_{zz}^{(1s)} = 0$ such that $\mathbf{C}_z^{(1s)} = \left[0 \; B_{zz}^{(1s)} \right]^T$. Coefficients $B_{zz}^{(1s)}$, and $A_{zz}^{(ns)}$ are the most important coefficients to be determined. All other coefficients will be expressed in terms of these two. Specifically, coefficients $\mathbf{C}_z^{(is)}$ will be expressed in terms of $B_{zz}^{(1s)}$, for $i = 1, ..., s-1, s$, and in terms of $A_{zz}^{(ns)}$, for $i = s, s+1, ..., n$.

Using the representation (14) and boundary and continuity conditions (20), (21), the coefficients $\mathbf{C}_z^{(is)}$ can be expressed in terms of the key coefficients $B_{zz}^{(1s)}$,

$$\begin{aligned} \mathbf{C}_z^{(1s)} &= B_{zz}^{(1s)}\Theta_z^1, \\ \mathbf{C}_z^{(is)} &= B_{zz}^{(1s)}\mathbf{L}_z^i - \frac{\delta_{is}}{2\gamma_s E_s}\left[0 \quad 1\right]^T, \end{aligned} \tag{22}$$

where $\Theta_z^1 = \left[0\ 1\right]^T$ and $\mathbf{L}_z^i = \Theta_z^{i,i-1}\cdot\Theta_z^{i-1,i-2}\cdot\ldots\cdot\Theta_z^{2,1}\cdot\Theta_z^1$, with $\Theta_z^{j+1,j}$ being (for $j = 1, 2, ..., n-1$),

$$\begin{aligned} \Theta_z^{j+1,j} \;=\; & \frac{1}{2T_{j+1}\varepsilon_j\gamma_{j+1}} \\ & \cdot\begin{bmatrix} T_{j+1}\left(\varepsilon_j\gamma_{j+1}+\varepsilon_{j+1}\gamma_j\right)T_j & T_{j+1}\left(\varepsilon_j\gamma_{j+1}-\varepsilon_{j+1}\gamma_j\right) \\ \left(\varepsilon_j\gamma_{j+1}-\varepsilon_{j+1}\gamma_j\right)T_j & \left(\varepsilon_j\gamma_{j+1}+\varepsilon_{j+1}\gamma_j\right) \end{bmatrix}. \end{aligned}$$

Similarly, we can express $\mathbf{C}_z^{(is)}$ in terms of the key coefficients $A_{zz}^{(ns)}$,

$$\begin{aligned} \mathbf{C}_z^{(ns)} &= A_{zz}^{(ns)}\Theta_z^n, \\ \mathbf{C}_z^{(is)} &= A_{zz}^{(ns)}\mathbf{R}_z^i - \frac{\delta_{is}E_s}{2\gamma_s T_s}\left[1 \quad 0\right]^T, \end{aligned} \tag{23}$$

where $\Theta_z^n = \left[1\ T_N\right]^T$ and $\mathbf{R}_z^i = (\Theta_z^{i+1,i})^{-1}\cdot(\Theta_z^{i+2,i+1})^{-1}\cdots(\Theta_z^{n,n-1})^{-1}\cdot\Theta_z^n$, with $(\Theta_z^{j+1,j})^{-1}$ being (for $j = 1, 2, ..., n-1$),

$$\begin{aligned} \left(\Theta_z^{j+1,j}\right)^{-1} \;=\; & \frac{1}{2T_j\varepsilon_{j+1}\gamma_j} \\ & \cdot\begin{bmatrix} \varepsilon_{j+1}\gamma_j+\varepsilon_j\gamma_{j+1} & \left(\varepsilon_{j+1}\gamma_j-\varepsilon_j\gamma_{j+1}\right)T_{j+1} \\ T_j\left(\varepsilon_{j+1}\gamma_j-\varepsilon_j\gamma_{j+1}\right) & T_j\left(\varepsilon_{j+1}\gamma_j+\varepsilon_j\gamma_{j+1}\right)T_{j+1} \end{bmatrix}. \end{aligned}$$

Equating the two different expressions for $\mathbf{C}_z^{(ss)}$, (22) and (23), we obtain the following system of matrix equations for the coefficients $A_{zz}^{(ns)}$ and $B_{zz}^{(1s)}$,

$$\begin{bmatrix} R^s_{z[1,1]} & -L^s_{z[1,1]} \\ R^s_{z[2,1]} & -L^s_{z[2,1]} \end{bmatrix}\begin{bmatrix} A_{zz}^{(ns)} \\ B_{zz}^{(1s)} \end{bmatrix} = \frac{1}{2\gamma_s}\begin{bmatrix} \frac{E_s}{T_s} \\ -\frac{1}{E_s} \end{bmatrix}, \tag{24}$$

where $R^s_{z[1,1]}$ and $R^s_{z[2,1]}$ are elements of the matrix $\mathbf{R}_z^s$ and $L^s_{z[1,1]}$ and $L^s_{z[2,1]}$ are elements of the matrix $\mathbf{L}_z^s$.

Once the system (24) is solved for $A_{zz}^{(ns)}$ and $B_{zz}^{(1s)}$, the remaining coefficients of (14) are obtained from equations (22) and (23).

When the point source is located in the first dielectric layer ($s = 1$), $A_{zz}^{(n1)} = \frac{E_1}{2\gamma_1 T_1 R^1_{z[1,\,1]}}$, and in the case when the source is in the last dielectric layer ($s = n$), $B_{zz}^{(1n)} = \frac{\frac{1}{E_n} + E_n}{2\gamma_n \left(L^n_{z[2,\,1]} - T_n L^n_{z[1,\,1]} \right)}$.

A similar procedure has been implemented to obtain DGFs (formulation is given in Appendix A) used in the magnetic-field integral equation formulation (4). In this case, different expressions for the eigenfunctions $\phi^{\alpha}_{mn}(x, y)$ and the transmission matrices Θ^n_x and $\Theta^{j+1,j}_x$ are used in the algorithm.

4. NUMERICAL RESULTS AND DISCUSSION

In this section, the behavior of the Green's function components $G^{(11)}_{xx,A1}(\mathbf{r}, \mathbf{r}')$ and $G^{(11)}_{zx,A1}(\mathbf{r}, \mathbf{r}')$ is investigated numerically for a two-layered, terminated rectangular waveguide with a point source arbitrarily located in region V_1, as shown in Fig. 4. One-dimensional characteristic Green's functions for this waveguide, derived using the procedure presented in Section 3, are given in Appendix B. Using equation (5) and the expressions of Appendix B, one can obtain the characteristic Green's functions for the DGFs of the electric type, published in [14]. Consequently, we were able to verify the accuracy of our new numerical code by using it to obtain the same results as we previously obtained in [14–16].

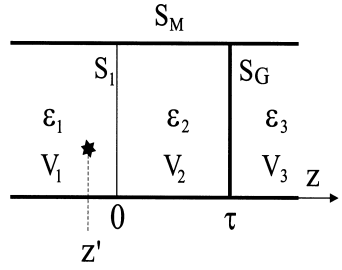

Figure 4. Two-layered, terminated rectangular waveguide with an arbitrarily oriented point source located in the region V_1.

The results are obtained at the frequency of 10 GHz for the following geometrical and material parameters: $a = 46$ mm, $b = 30.5$ mm, $\tau = 0.7874$ mm, $\varepsilon_1 = 1$, and $\varepsilon_2 = 2.2$, with a point source located

at $(x', y', z') = (0.5a, 0.5b, 0)$. Observation points are first taken along the diagonal line $y = xb/a$ at the dielectric interface of regions V_1 and V_2 at $z = 0$. In the double infinite series expansion (9) for the Green's function components $G^{(11)}_{\alpha\beta,A1}$, each of the indexes m and n ranges from 0 to ∞. However, in a practical simulation, we truncated this representation at a maximum value of m and n denoted by M. Figs. 5(a) and 5(b) show the behavior of the real part of the Green's function component $G^{(11)}_{xx,A1}(\mathbf{r}, \mathbf{r}')$ versus truncation variable M for different observation point positions. Particularly, the observation point (x, y, z) in Fig. 5(a) varies from the point $(0.35a, 0.35b, 0)$ to the point $(0.46a, 0.46b, 0)$, while in Fig. 5(b) it varies further toward the source point, starting at the position $(0.48a, 0.48b, 0)$ and ending at the position $(0.497a, 0.497b, 0)$. Note that the y-axis values in Fig. 5(b) are more than an order of magnitude larger than those in Fig. 5(a). As can be seen from these figures, as the observation point approaches the source point, the convergence of the Green's function component becomes slower. Specifically, we observe an oscillatory behavior of the DGF component with the oscillations becoming slower in the source region, requiring a larger value of M for an accurate approximation. Similarly, the behavior of the real part of the Green's function component $G^{(11)}_{zx,A1}(\mathbf{r}, \mathbf{r}')$ versus M is shown in Figs. 6(a) and 6(b), for the same set of observation point positions. As can be seen, the component $G^{(11)}_{zx,A1}(\mathbf{r}, \mathbf{r}')$ shows a similar convergence behavior, except that the curves in the Figs. 6(a) and 6(b) are more corrugated than those depicted in Figs. 5(a) and 5(b).

Finally, observation points are taken along the line $(x, y) = (0.475a, 0.475b)$ and convergence of the real parts of the Green's function components $G^{(11)}_{xx,A1}(\mathbf{r}, \mathbf{r}')$ and $G^{(11)}_{zx,A1}(\mathbf{r}, \mathbf{r}')$ is shown in Figs. 7 and 8, respectively, for different z-coordinate values. Again, it can be seen, that convergence of the Green's function components becomes slower as the observation point approaches into the source region at $z = 0$. Specifically, less than $M^2 = 100^2$ terms is needed for an accurate approximation of the DGF components in the expansion (9) for $z \leq -0.5\tau$ (see the curves for $z = -4\tau, -3\tau, -2\tau, -1\tau, -0.5\tau$ in Figs. 7 and 8). However, the corresponding value of the variable M increases drastically as the observation point approaches further towards the source point (see the curves for $z = -0.25\tau, 0$ in Figs. 7 and 8).

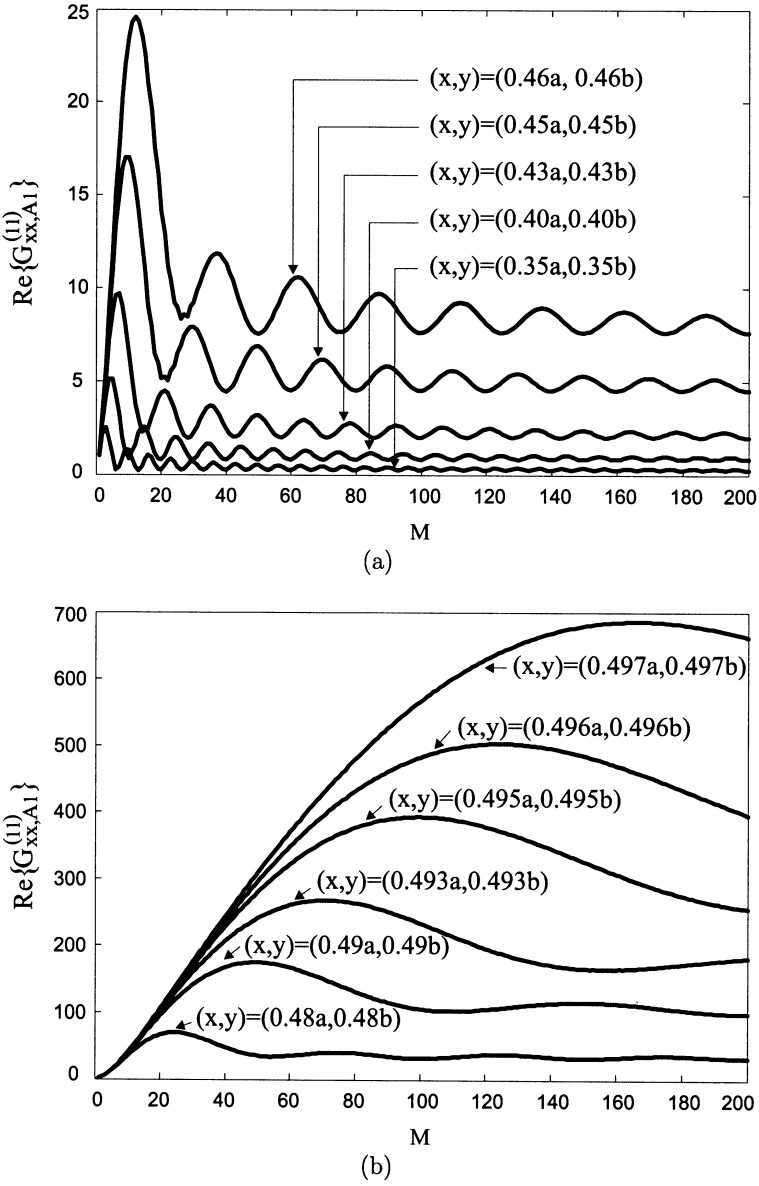

Figure 5. Convergence of the DGF component, $G^{(11)}_{xx,A1}$, for two-layered, terminated rectangular waveguide for various positions of the observation point (x, y) at dielectric interface $(z = 0)$.

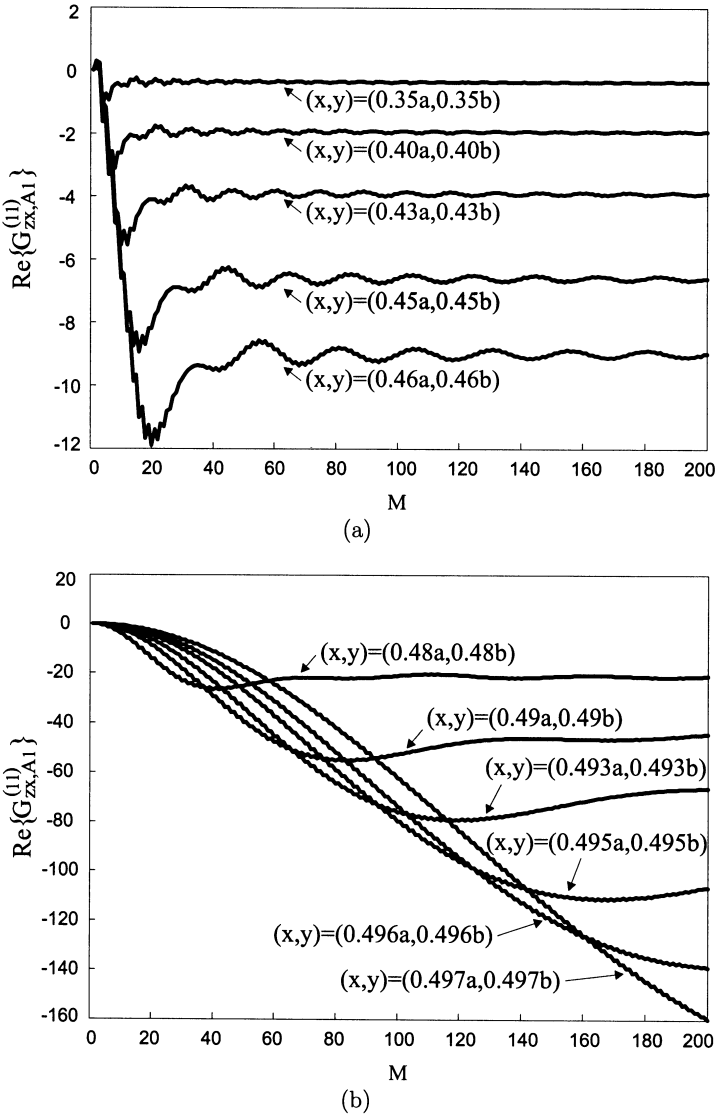

Figure 6. Convergence of the DGF component, $G^{(11)}_{zx,A1}$, for two-layered, terminated rectangular waveguide for various positions of the observation point (x, y) at dielectric interface $(z = 0)$.

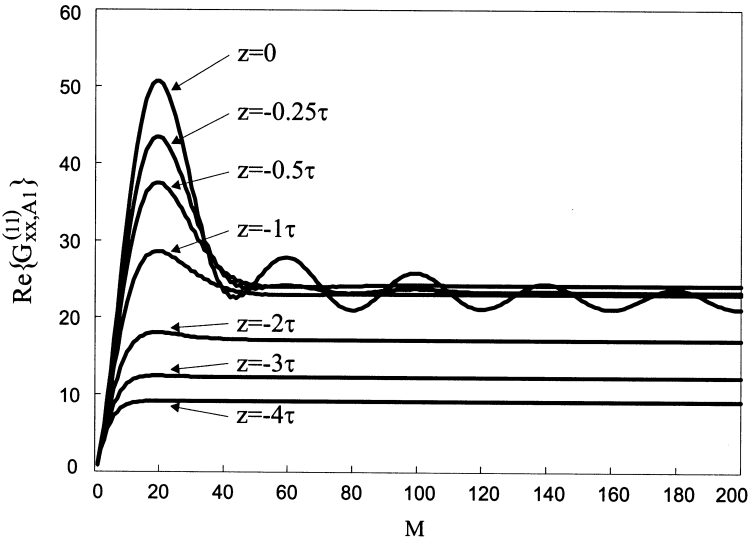

Figure 7. Convergence of the DGF component, $G^{(11)}_{xx,A1}$, for two-layered, terminated rectangular waveguide for various positions of the observation point along the waveguide.

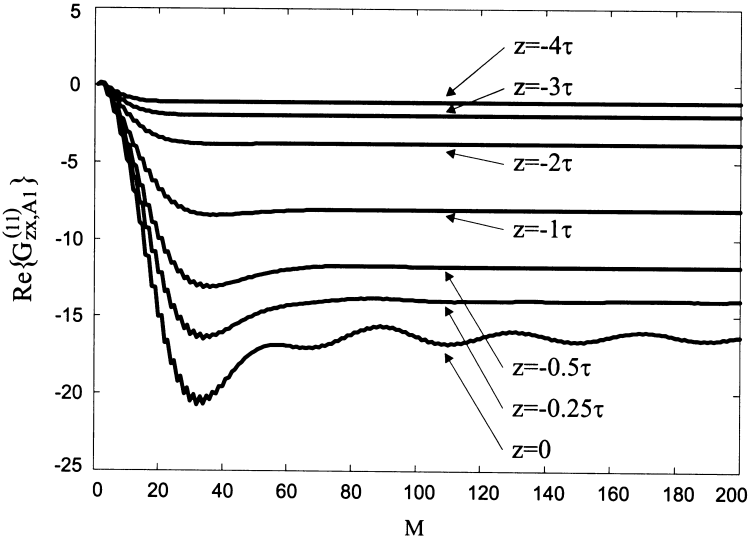

Figure 8. Convergence of the DGF component, $G^{(11)}_{zx,A1}$, for two-layered, terminated rectangular waveguide for various positions of the observation point along the waveguide.

5. CONCLUSION

A full-wave integral equation formulation and magnetic potential Green's dyadics for a multilayered rectangular waveguide are presented for modeling printed antenna arrays used in waveguide-based spatial power combiners. The Green's functions are derived in the form of a partial eigenfunction expansion as a double series over the complete system of eigenfunctions of the transverse Laplacian operator. The three-dimensional problem for DGF components is reduced to a one-dimensional Sturm-Liouville boundary value problem for the characteristic Green's functions in the waveguiding direction. These functions are then obtained in the closed form as a superposition of primary and scattered parts. The amplitude coefficients of forward and backward traveling waves in the scattered Green's function in different dielectric layers are obtained as a product of transmission matrices of corresponding layers. Numerical results are shown for the convergence of the Green's function components for a two-layered, terminated rectangular waveguide with an arbitrarily oriented point source.

APPENDIX A. MAGNETIC POTENTIAL GREEN'S DYADICS FOR A SEMI-INFINITE MULTILAYERED RECTANGULAR WAVEGUIDE USED IN THE MAGNETIC-FIELD INTEGRAL EQUATION FORMULATION

The magnetic potential DGF for a semi-infinite multilayered rectangular waveguide shown in Fig. 3 satisfies the system of dyadic differential equations in dielectric regions V_i (for $i = 1, 2, ..., n$),

$$\nabla^2 \underline{\mathbf{G}}_{A2}^{(in)}\left(\mathbf{r}, \mathbf{r}'\right) + k_i^2 \underline{\mathbf{G}}_{A2}^{(in)}\left(\mathbf{r}, \mathbf{r}'\right) = -\delta_{in} \underline{\mathbf{I}} \delta\left(\mathbf{r} - \mathbf{r}'\right), \quad \mathbf{r} \in V_i, \tag{A1}$$

subject to boundary conditions of the second kind on the waveguide surface S_M and surface of the ground plane S_G,

$$\begin{gathered} \hat{n} \times \nabla \times \underline{\mathbf{G}}_{A2}^{(in)}\left(\mathbf{r}, \mathbf{r}'\right) = 0, \quad \mathbf{r} \in S_M \cup S_G \\ \hat{n} \cdot \left(\underline{\mathbf{I}} + \tfrac{1}{k_i^2} \nabla\nabla\right) \cdot \underline{\mathbf{G}}_{A2}^{(in)}\left(\mathbf{r}, \mathbf{r}'\right) = 0, \quad \mathbf{r} \in S_M \cup S_G \end{gathered} \tag{A2}$$

and mixed continuity conditions of the third kind across the dielectric interfaces S_q (for $q = 1, 2, ..., n-1$),

$$\begin{aligned}
\hat{z} \times \underline{\mathbf{G}}_{A2}^{(qn)}\left(\mathbf{r}, \mathbf{r}'\right) &= \hat{z} \times \underline{\mathbf{G}}_{A2}^{(q+1n)}\left(\mathbf{r}, \mathbf{r}'\right), && \mathbf{r} \in S_q \\
\frac{1}{\varepsilon_q} \hat{z} \cdot \underline{\mathbf{G}}_{A2}^{(qn)}\left(\mathbf{r}, \mathbf{r}'\right) &= \frac{1}{\varepsilon_{q+1}} \hat{z} \cdot \underline{\mathbf{G}}_{A2}^{(q+1n)}\left(\mathbf{r}, \mathbf{r}'\right), && \mathbf{r} \in S_q \\
\frac{1}{\varepsilon_q} \hat{z} \times \nabla \times \underline{\mathbf{G}}_{A2}^{(qn)}\left(\mathbf{r}, \mathbf{r}'\right) &= \frac{1}{\varepsilon_{q+1}} \hat{z} \times \nabla \times \underline{\mathbf{G}}_{A2}^{(q+1n)}\left(\mathbf{r}, \mathbf{r}'\right), && \mathbf{r} \in S_q \\
\frac{1}{\varepsilon_q} \nabla \cdot \underline{\mathbf{G}}_{A2}^{(qn)}\left(\mathbf{r}, \mathbf{r}'\right) &= \frac{1}{\varepsilon_{q+1}} \nabla \cdot \underline{\mathbf{G}}_{A2}^{(q+1n)}\left(\mathbf{r}, \mathbf{r}'\right), && \mathbf{r} \in S_q.
\end{aligned} \tag{A3}$$

APPENDIX B. CHARACTERISTIC GREEN'S FUNCTIONS FOR A TWO-LAYERED, TERMINATED RECTANGULAR WAVEGUIDE

For the special case of a two-layered, terminated rectangular waveguide with a point source arbitrarily located in the first dielectric layer (region V_1 in Fig. 4), one-dimensional characteristic Green's functions are obtained as follows,

$$\begin{aligned}
f_{mn,xx}^{(11)}\left(z, z'\right) &= f_{mn,yy}^{(11)}\left(z, z'\right) \\
&= \frac{e^{-\gamma_1 |z - z'|}}{2\gamma_1} + e^{\gamma_1 (z + z')} \left(\frac{1}{Z_o^{TE}} - \frac{1}{2\gamma_1} \right),
\end{aligned} \tag{B1}$$

$$f_{mn,zx}^{(11)}\left(z, z'\right) = e^{\gamma_1 (z + z')} \frac{k_x \left(\dfrac{\varepsilon_2}{\varepsilon_1} - 1 \right)}{Z_o^{TE} Z_e^{TM}}, \tag{B2}$$

$$f_{mn,zy}^{(11)}\left(z, z'\right) = e^{\gamma_1 (z + z')} \frac{k_y \left(\dfrac{\varepsilon_2}{\varepsilon_1} - 1 \right)}{Z_o^{TE} Z_e^{TM}}, \tag{B3}$$

$$f_{mn,zz}^{(11)}\left(z, z'\right) = \frac{e^{-\gamma_1 |z - z'|}}{2\gamma_1} + e^{\gamma_1 (z + z')} \left(\frac{\frac{\varepsilon_2}{\varepsilon_1}}{Z_e^{TM}} - \frac{1}{2\gamma_1} \right), \tag{B4}$$

$$f_{mn,xx}^{(21)}\left(z, z'\right) = f_{mn,yy}^{(21)}\left(z, z'\right) = e^{\gamma_1 z'} \frac{\sinh\left(\gamma_2 \left(\tau - z\right)\right)}{Z_o^{TE} \sinh\left(\gamma_2 \tau\right)}, \tag{B5}$$

$$f_{mn,zx}^{(21)}\left(z, z'\right) = e^{\gamma_1 z'} \frac{k_x \left(\dfrac{\varepsilon_2}{\varepsilon_1} - 1 \right) \cosh\left(\gamma_2 \left(\tau - z\right)\right)}{Z_o^{TE} Z_e^{TM} \cosh\left(\gamma_2 \tau\right)}, \tag{B6}$$

$$f^{(21)}_{mn,zy}\left(z,z'\right) = e^{\gamma_1 z'} \frac{k_y \left(\dfrac{\varepsilon_2}{\varepsilon_1} - 1\right) \cosh\left(\gamma_2\left(\tau - z\right)\right)}{Z_o^{TE} Z_e^{TM} \cosh\left(\gamma_2 \tau\right)}, \tag{B7}$$

$$f^{(21)}_{mn,zz}\left(z,z'\right) = e^{\gamma_1 z'} \frac{\dfrac{\varepsilon_2}{\varepsilon_1} \cosh\left(\gamma_2\left(\tau - z\right)\right)}{Z_e^{TM} \cosh\left(\gamma_2 \tau\right)}, \tag{B8}$$

where Z_o^{TE} and Z_e^{TM} represent the characteristic dispersion functions of TE odd and TM even modes of a grounded dielectric slab of thickness τ bounded with the electric walls at $x = 0, a$ and $y = 0, b$,

$$Z_o^{TE} = \gamma^{(1)}_{mn} + \gamma^{(2)}_{mn} \coth \gamma^{(2)}_{mn} \tau,$$
$$Z_e^{TM} = \frac{\varepsilon_2}{\varepsilon_1} \gamma^{(1)}_{mn} + \gamma^{(2)}_{mn} \tanh \gamma^{(2)}_{mn} \tau.$$

REFERENCES

1. Collin, R. E., *Field Theory of Guided Waves*, IEEE Press, New Jersey, 1991.
2. Tai, C. T., *Dyadic Green's Functions in Electromagnetic Theory*, IEEE Press, New Jersey, 1993.
3. Li, L. W., P. S. Kooi, M. S. Leong, T. S. Yeo, and S. L. Ho, "On the eigenfunction expansion of electromagnetic dyadic Green's functions in rectangular cavities and waveguides," *IEEE Trans. Microwave Theory Tech.*, Vol. 43, 700–702, March 1995.
4. Tai, C. T. and P. Rozenfeld, "Different representations of dyadic Green's functions for a rectangular cavity," *IEEE Trans. Microwave Theory Tech.*, Vol. 24, 597–601, Sept. 1976.
5. Wu, D. I. and D. C. Chang, "Hybrid representation of the Green's function in an overmoded rectangular cavity," *IEEE Trans. Microwave Theory Tech.*, Vol. 36, 1334–1342, Sept. 1988.
6. Jin, H. and W. Lin, "Dyadic Green's functions for a rectangular waveguide with an E-plane dielectric slab," *IEE Proc, Microwaves, Ant and Propagat.*, Vol. 137, 231–234, Aug. 1990.
7. Fang, D. G., F. Ling, and Y. Long, "Rectangular waveguide Green's function involving complex images," *IEEE AP-S Int. Symp. Dig.*, Vol. 2, 1045–1048, June 1995.
8. Gentili, G. G., L. E. G. Castillo, M. S. Palma, and F. P. Martinez, "Green's function analysis of single and stacked rectangular microstrip patch antennas enclosed in a cavity," *IEEE Trans. on Antennas and Propagat.*, Vol. 45, 573–579, Apr. 1997.

9. Park, M. J. and S. Nam, "Rapid summation of the Green's function for the rectangular waveguide," *IEEE Trans. Microwave Theory Tech.*, Vol. 46, 2164–2166, Dec. 1998.
10. Marliani, F. and A. Ciccolella, "Computationally efficient expressions of the dyadic Green's function for rectangular enclosures," *Journal of Electromagnetic Waves and Applications*, Vol. 14, 1635–1636, 2000.
11. Jin, H., W. Lin, and Y. Lin, "Dyadic Green's functions for rectangular waveguide filled with longitudinally multilayered isotropic dielectric and their application," *IEE Proceedings: Microwaves, Ant. and Prop.*, Vol. 141, No. 6, 504–508, Dec. 1994.
12. Li, L. W., P. S. Kooi, M. S. Leong, T. S. Yeo, and S. L. Ho, "Input impedance of a probe-excited semi-infinite rectangular waveguide with arbitrary multilayered loads: part I - dyadic Green's functions," *IEEE Trans. Microwave Theory Tech.*, Vol. 43, 1559–1566, July 1995.
13. Felsen, L. B. and N. Marcuvitz, *Radiation and Scattering of Waves*, IEEE Press, New Jersey, 1994.
14. Yakovlev, A. B., S. Ortiz, M. Ozkar, A. Mortazawi, and M. B. Steer, "Electric dyadic Green's functions for modeling resonance and coupling effects in waveguide-based aperture-coupled patch arrays," *ACES Journal*, Vol. 17, No. 2, 123–133, July 2002.
15. Yakovlev, A. B., A. I. Khalil, C. W. Hicks, A. Mortazawi, and M. B. Steer, "The generalized scattering matrix of closely spaced strip and slot layers in waveguide," *IEEE Trans. Microwave Theory Tech.*, Vol. 48, 126–137, Jan. 2000.
16. Yakovlev, A. B., S. Ortiz, M. Ozkar, A. Mortazawi, and M. B. Steer, "A waveguide-based aperture-coupled patch amplifier array: Full-wave system analysis and experimental validation," *IEEE Trans. Microwave Theo. Tech.*, Vol. 48, 2692–2699, 2000.
17. Huang, C. P., A. Z. Elsherbeni, and C. E. Smith, "Analysis and design of tapered meander line antennas for mobile communications," *ACES Journal*, Vol. 15, No. 3, 159–166, 2000.
18. Huang, C. P., J. B. Chen, A. Z. Elsherbeni, and C. E. Smith, "FDTD characterization of meander line antennas for RF and wireless communications," *Eelectromagnetic Wave Monograph Series, Progress in Electromagnetic Research (PIER 24)*, Vol. 24, Ch. 9, 257–277, 1999.
19. Hanson, G. W. and A. B. Yakovlev, *Operator Theory for Electromagnetics: An Introduction*, Springer-Verlag, New York, NY, Oct. 2001.